Journal of Alloys and Compounds 509 (2011) 7607–7610

Contents lists available at ScienceDirect

Journal of Alloys and Compounds

journal homepage: www.elsevier.com/locate/jallcom

The twin mechanism of Portevin Le Chatelier in Mg–5Li–3Al–1.5Zn–2RE alloy

T.Q. Li[a], Y.B. Liu[a], Z.Y. Cao[a,*], R.Z. Wu[b], M.L. Zhang[b], L.R. Cheng[a], D.M. Jiang[a]

[a] The Key Laboratory of Automobile Materials, Ministry of Education, Department of Materials Science and Engineering, Jilin University, No. 5988 Renmin Street, Changchun 130025, PR China
[b] Key Laboratory of Superlight Materials and Surface Technology, Ministry of Education, Harbin Engineering University, 145 Nantong Street, Harbin 150001, PR China

ARTICLE INFO

Article history:
Received 14 September 2010
Received in revised form 18 April 2011
Accepted 19 April 2011
Available online 27 April 2011

Keywords:
Metals and alloys
Mechanical properties
Microstructure
Twinning
Portevin Le Chatelier effect

ABSTRACT

The small serrated flow, severe Portevin Le Chatelier (PLC) phenomenon and abnormal strain rate sensitivity (SRS) were observed from the tensile curves of extruded Mg–5Li–3Al–1.5Zn–2RE alloy. The serrated curves were investigated by optical microscopy, step-tensile test and transmission electron microscopy. The small serrated flow is due to the traditional dynamic strain ageing. The positive SRS is caused by dynamic strain ageing. The severe Portevin Le Chatelier phenomenon and the negative SRS are attributed to a larger number of twins. Transmission electron microscope diffraction pattern reveals the $\{10\bar{1}2\}$ twin and $\{10\bar{1}1\}$ twins.

1. Introduction

Mg–Li alloy has low density, known as the lightest metallic engineering materials. It also shows high specific stiffness, high electrical and thermal conductivities [1–4]. In the fields of aerospace, military hardware and exactitude apparatus, Mg–Li base alloys were used widely. In order to obtain better mechanical properties, Al, Zn, and rare earth elements are often used as an alloying element in Mg–Li base alloys [3–5]. The addition of Li decreases the *c*/*a* value of HCP lattice of magnesium solid solution and improves the plasticity property of alloys. Most commonly, Al and Zn are the two alloying elements that are used in magnesium alloys. The addition of these elements can strengthen the Mg–Li alloys. Furthermore, the addition of rare earth elements can refine the microstructure, and the mechanical properties of magnesium alloys can be improved further.

The stress–strain curve which displays a wavy profile or serrated flow of a deforming alloy is known as the Portevin Le Chatelier (PLC) effect. The PLC effect is basically understood as a material intrinsic property with the local phenomena referred to as dynamic strain ageing (DSA) [6–8], and it may induce macroscopic negative strain rate sensitivity (SRS) [9]. The irregular plastic flow is a reflection of material instability and associated inhomogeneous deformation (strain localization). The PLC effect has been investigated extensively in the face-centered cubic and body-centered cubic alloys, such as aluminum alloys, iron alloys, and steel alloys. However, much less attention is paid to magnesium alloys which possess the close-packed hexagonal structure (HCP) [9–11]. The special Portevin Le Chatelier effect was found in Mg–5Li–3Al–1.5Zn–2RE alloy, which has important link with the microstructure.

As for the Mg–Li base alloys is concerned, the research about the PLC has not been reported in the literature. In the current study, the small serrated flow and severe PLC phenomenon were found in the tensile test of Mg–5Li–3Al–1.5Zn–2RE (LAZ532-2RE) alloy. The aim of this work was to investigate the relationship between the observed severe PLC effect and the microstructure in LAZ532-2RE alloy. The detailed analysis on the PLC phenomenon and abnormal strain rate sensitivity in LAZ532-2RE alloy were reported in this paper.

2. Experimental details

Melting of the LAZ532-2RE alloy was conducted in an induction furnace (ZG-0.01) in argon atmosphere. Then the cylindrical specimens were annealed 12 h at 523 K and the specimens were extruded at 553 K. The diameter of specimens after extrusion was changed from 55 mm to 13 mm. Both the designed melt compositions and the chemical compositions of the samples measured by inductive coupled plasma (ICP) are listed in Table 1.

The tensile specimens, with gauge dimensions of $10 \times 4 \times 1.5$ mm, were taken from the extruded rods. The specimen surfaces were grounded up to 2000 grid SiC paper. The tensile tests were carried out using MTS810 tensile testing machine under various strain rates ranging from 1×10^{-4} to $1 \times 10^{-2} s^{-1}$. The results of tensile tests were based on the average data of three or four specimens on each test condition.

The samples were carefully ground and polished, then etched in 4 vol% nitric acid plus ethanol solution. The microstructures near the fractured surfaces were observed by Olympus-PMG3 to investigate the relationship between microstructure and the PLC effect. Transmission electron microscope (JEM-2000EX)

* Corresponding author. Tel.: +86 431 8509 5874; fax: +86 431 8509 5874.
E-mail address: caozy@jlu.edu.cn (Z.Y. Cao).

0925-8388/$ – see front matter © 2011 Elsevier B.V. All rights reserved.
doi:10.1016/j.jallcom.2011.04.099

Table 1
The designed melt compositions and the chemical compositions of the samples.

	Li	Al	Zn	RE (La–Pr–Ce)
Designation composition (mass%)	5	3	1.5	2
Analyzed composition (mass%)	5.12	3.07	1.45	1.57La–0.086Pr–0.12Ce

was also employed to observe the microstructure and measure the diffraction pattern of the specimens. The *c*/*a* (lattice constant ratio) value of α-Mg was calculated from the X-ray diffraction (D/Max2500PC Rigaku, Japan) step-scanning results.

3. Results

3.1. Tensile test and microstructures

Fig. 1(a) shows the engineering stress–strain curves of LAZ532-2RE alloy under different strain rates at 293 K. In order to observe the relationship between the PLC phenomenon and the strain rate, the curves of engineering stress–strain were separated by artificially. It is obvious that the fluctuation of PLC effect becomes smaller with the increase of strain rate. The severe PLC effect can be observed in the middle section of stress–strain curves for each strain rate. From Fig. 1(b)–(f), a large number of twins can be observed and the quantity of twins increases with the strain rate. A certain angle exists between the direction of twin and the tensile direction (the arrow shows the tensile direction).

3.2. Step-tensile test and twin observation

Fig. 2 indicates the relationship between the PLC effects and the deformation twins. There is almost no twin in Fig. 2(b). When the severe PLC effect occurs in the curve, the twins were observed in Fig. 2(c). According to Fig. 2(b)–(d), the quantity of twins increases with tensile test proceeding. It can be concluded that the severe PLC phenomenon has important links with the twins.

4. Discussions

4.1. Strain rate dependencies of tensile properties

Fig. 3(a) shows the abnormal SRS curve. The strain rate sensitivity *m* can be estimated using the following equation:

$$m = \frac{\partial \ln \sigma}{\partial \ln \varepsilon} \quad (1)$$

where m is the strain rate sensitivity, σ is the strength, and ε is the strain. The critical strain rate ($\dot{\varepsilon}_c$) is $1 \times 10^{-3}\ s^{-1}$. For $\dot{\varepsilon} < \dot{\varepsilon}_c$, the predominant mechanism is dynamic strain ageing. When the strain rate exceeds $\dot{\varepsilon}_c$, larger burst of plastic strain due to the twin shear transformation makes the tensile strength decline slightly.

Fig. 3(b) provides more details on the severe PLC. Between two large serrated flows (severe PLC), small serrated flows can be observed. The large serrated flows have a special shape with a sudden drop followed by a slow rise. It is evident that the shear deformation twins supply a certain amount of strain in a very short time, with the tensile test proceeding, the stress increases slowly

4.2. The deformation twin mechanism of PLC effect

In Fig. 3(c), the ideal simulate curve is drawn to elucidate the severe PLC effect. The following assumed equation is employed to elucidate the relationship between the shapes of PLC effect and strain rate:

$$t = \frac{nd}{\dot{\varepsilon}} \quad (2)$$

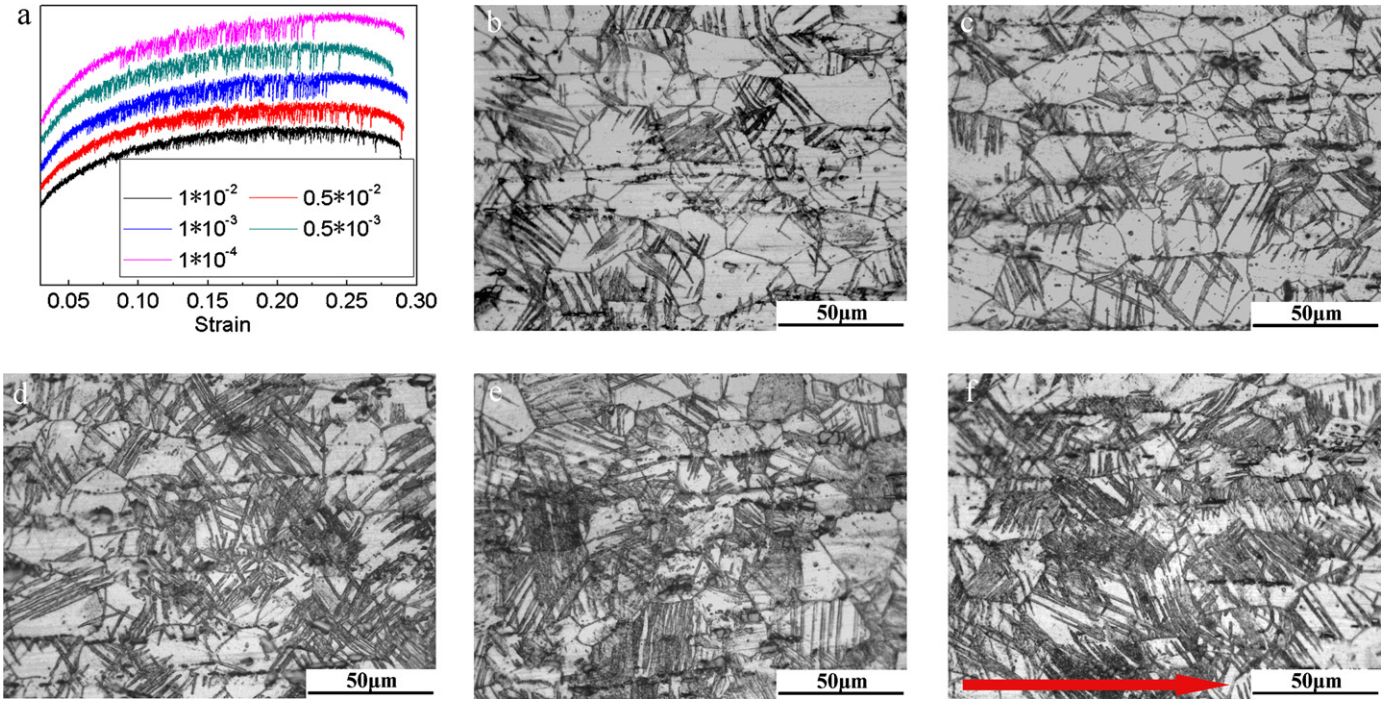

Fig. 1. (a) The engineering stress–strain curves of LAZ532-2RE alloy (separated by artificially); microstructures near the fractured surfaces of specimens after tensile test at different strain rate: (b) 1×10^{-4}, (c) 0.5×10^{-3}, (d) 1×10^{-3}, (e) 0.5×10^{-2}, (f) 1×10^{-2}.

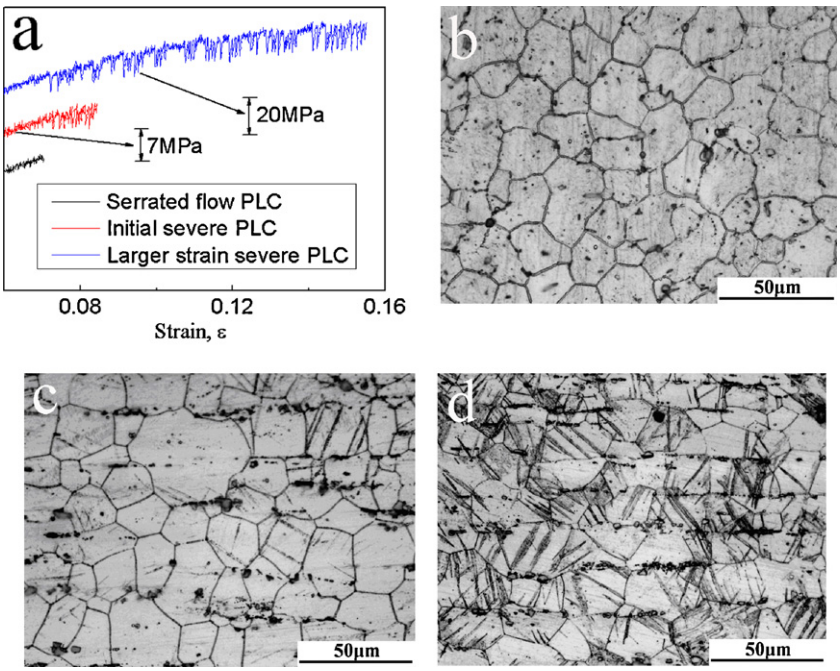

Fig. 2. (a) The step-tensile test at the strain rate of 1×10^{-3}; (b) the microstructure of serrated flow PLC effect; (c) initial severe PLC effect; (d) the larger strain severe PLC effect.

where t is the time span from the A to C, n is the number of shear transformation twin, d is the strain of one twin supplied and the $\dot{\varepsilon}$ is the strain rate. Accordingly, a certain number of twins supply the strain $\varepsilon_{AC} = \varepsilon_C - \varepsilon_A = nd$, and the time t decreases with the strain rate increasing. Therefore, the serrated span becomes smaller as the strain rate increases. This causes the different types of PLC curves. Jiang et al. [12] reported that the different types of the PLC effect (types A, B and C) are attributed to the mobile dislocation with the mobility of solute diffusion and strain rate. While in this research, as for the LAZ532-2RE alloy is concerned, the different types of PLC effects are attributed to the shearing deformation twin and the strain rate.

Table 2 shows the statistics of the volume fraction of twins, $\varepsilon_{AC} = nd$ and the tensile strength declines $\Delta\sigma_{AB} = \sigma_A - \sigma_B$. The volume fractions of twins were calculated by the OLYCTA m3 software. The ε_{AC} and $\Delta\sigma_{AB}$ are both averaged from ten data. From Table 2, the quantity of twins increases with the strain rate. More twins mean supplying larger strain, but a certain amount of twins cause a tiny strain ε_{AC} and the strain rate changes twenty times. Therefore, the strain rate has a stronger impact than the quantity of twins. Both ε_{AC} and $\Delta\sigma_{AB}$ decrease as the strain rate increasing. Those statistics prove that the different types of PLC effect are attributed to the deformation twin and the strain rate.

4.3. Analysis of the twins in LAZ532-2RE alloy

The close-packed plane, slip plane, of magnesium is 0001 and the c/a value of Mg is 1.624 (from the jade 5.0 soft (PDF#35-0821)). Lithium decreases lattice parameters of Mg, particularly remarkably reduces c constant. The c/a value of α-Mg in the LAZ532-2RE alloy is 1.6074 according to the X-ray step-scanning results. The non-basal (prismatic plane and pyramidal plane) slip becomes easy. Ando et al. [13] reported the Mg–Li (3.5–14%) alloy come forth pyramidal slip $\{11\bar{2}2\} < 11\bar{2}3 >$ at 77–293 K. The elongation of LAZ531-2RE is greater than that of AZ31 [14,15]. Twin plays an important role during the plastic deformation [16,17].

Fig. 4(a) shows the typical microstructure and diffraction pattern of the $\{10\bar{1}2\}$ twin. The arrows in the figure indicate the twin interfaces. A diffraction pattern taken from the twinned region is shown in Fig. 4(a). The twin and the matrix are related by 86° rotation around the $\{1\bar{2}10\}$ and the twinning plane is $\{10\bar{1}2\}$ [18]. The TEM image of the $\{10\bar{1}1\}$ twin and diffraction pattern are shown in Fig. 4 (b). The c-axes of the twin and the matrix are rotated by 56° around the $< 1\bar{2}10 >$ direction [18]. Analysis of the diffraction pattern indicates that the twin plane is $\{10\bar{1}1\}$ twin.

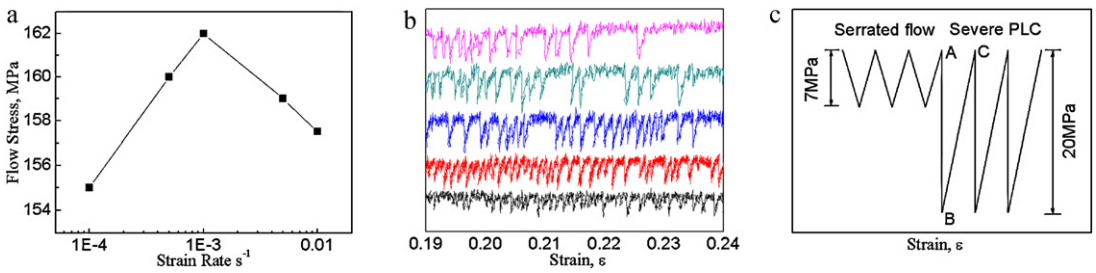

Fig. 3. (a) The strain rate vs. the flow stress; (b) the drawing of partial enlargement of Fig. 1(a); (c) the ideal simulate curve of serrated flow and severe PLC effect.

Table 2
The statistics of the volume fraction of twins, ε_{AC} and $\Delta\sigma_{AB}$.

Strain rate, s^{-1}	1×10^{-4}	0.5×10^{-3}	1×10^{-3}	0.5×10^{-2}	1×10^{-2}
Volume fraction of twins in Fig. 1(b)–(f)	39%	41.45%	51.13%	56.09%	59.4%
$\varepsilon_{AC} = \varepsilon_C - \varepsilon_A$	0.0012	0.001	0.00095	0.00085	0.00067
$\Delta\sigma_{AB} = \sigma_A - \sigma_B$	19	20	17	15	12

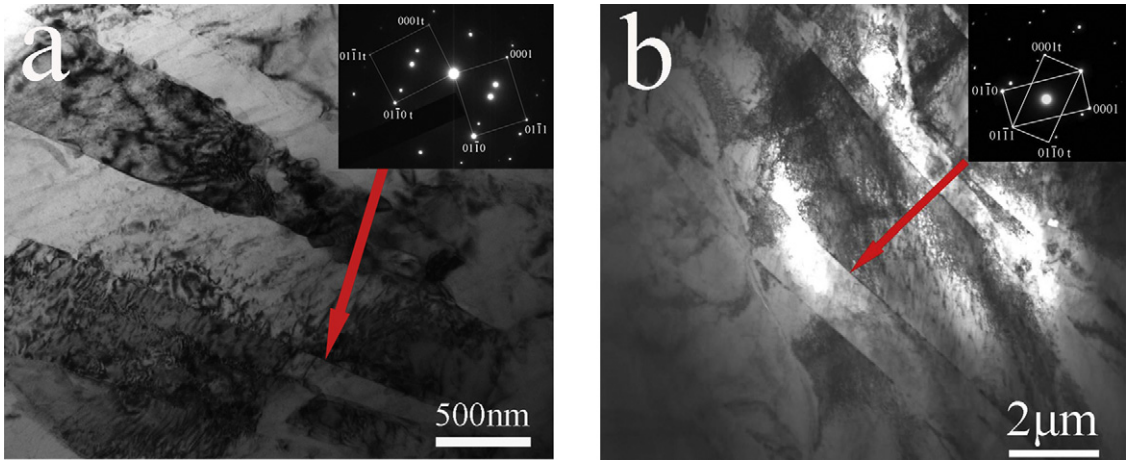

Fig. 4. (a) and (b) TEM micrographs and diffraction pattern of the different twins at strain rate 1×10^{-2}.

5. Conclusions

In summary, the serrated flow, severe PLC effect and abnormal SRS were observed in LAZ532-2RE alloy. The small serrated flow is due to the traditional dynamic strain ageing. The positive SRS is caused by dynamic strain ageing, and the negative SRS is attributed to the larger burst of plastic strain coming from the twin shear transformation. The severe PLC phenomenon is caused by a large number of twins. Due to the addition of Lithium in LAZ532-2RE alloy, the c/a value of α-Mg decreased from 1.624 to 1.6074. The non-basal slip was easily activated at room temperature. Accordingly, a larger number of twins were observed in the specimens after the tensile test. Analysis of the diffraction pattern indicates the $\{10\bar{1}2\}$ twin and $\{10\bar{1}1\}$ twin.

Acknowledgements

This study is supported by the National Science and Technology supporting program of China (Nos. 2006BA104B04-1; 2006BAE04B07-03). The Science and Technology Supporting Project of Changchun City (No. 2007KZ05), and the "985 Project" of Jilin University.

References

[1] T. Zhou, H. Xia, M.B. Yang, Z.M. Zhou, K. Chen, J.J. Hu, Z.H. Chen, J. Alloys Compd. 509 (2011) L145–L149.
[2] J.Q. Li, Z.K. Qu, R.Z. Wu, M.L. Zhang, J.H. Zhang, Mater. Sci. Eng. A 528 (2011) 3915–3920.
[3] H.W. Dong, L.D. Wang, Y.M. Wu, L.M. Wang, J. Alloys Compd. 506 (2010) 468–474.
[4] R.Z. Wu, Y.S. Deng, M.L. Zhang, J. Mater. Sci. 44 (2009) 4132–4139.
[5] J.H. Zhang, Z. Leng, M.L. Zhang, J. Meng, R.Z. Wu, J. Alloys Compd. 509 (2011) 1069–1078.
[6] A.H. Cottrell, Oxford University Press, (1953) p. 208.
[7] J.D. Baird, American Society of Metals, Metals Park (OH, USA), (1973) p. 1191.
[8] A. Van den Beukel, Phys. Status Solidi A 30 (1975) 197–206.
[9] C. Wang, Y.B. Xu, E.H. Han, Mater. Lett. 60 (2006) 2941–2944.
[10] C. Corby, C.H. Cáceres, P. Lukáè, Mater. Sci. Eng. A 387–389 (2004) 22–24.
[11] S.M. Zhu, J.F. Nie, Scripta Mater. 50 (2004) 51.
[12] H.F. Jiang, Q.C. Zhang, X.D. Chen, Z.J. Chen, Z.Y. Jiang, X.P. Wu, et al., Acta Mater. 55 (2007) 2219–2228.
[13] S. Ando, M. Tanaka, H. Tonda, Mater. Sci. Forum. 87 (2003) 419–422.
[14] H.W. Lee, T.S. Lui, L.H. Chen, J. Alloys Compd. 475 (2009) 139–144.
[15] R.Z. Wu, Z.K. Qu, M.L. Zhang, Rev. Adv. Mater. Sci. 24 (2010) 14–34.
[16] B. Li, E. Ma, Acta Mater. 57 (2009) 1734–1743.
[17] M.R. Barnett, Mater. Sci. Eng. A 464 (2007).
[18] D. Ando, J. Koike, Y. Sutou, Acta Mater. 58 (2010) 4316–4324.